

ANIMC: A Soft Framework for Auto-weighted Noisy and Incomplete Multi-view Clustering

Xiang Fang, Yuchong Hu, *Member, IEEE*, Pan Zhou, *Member, IEEE*, Xiao-Yang Liu, *Graduate Student Member, IEEE*, and Dapeng Oliver Wu, *Fellow, IEEE*

Abstract—Multi-view clustering has wide applications in many image processing scenarios. In these scenarios, original image data often contain missing instances and noises, which is ignored by most multi-view clustering methods. However, missing instances may make these methods difficult to use directly and noises will lead to unreliable clustering results. In this paper, we propose a novel Auto-weighted Noisy and Incomplete Multi-view Clustering framework (ANIMC) via a *soft* auto-weighted strategy and a doubly *soft* regular regression model. Firstly, by designing adaptive semi-regularized nonnegative matrix factorization (adaptive semi-RNMF), the soft auto-weighted strategy assigns a *proper* weight to each view and adds a soft boundary to balance the influence of noises and incompleteness. Secondly, by proposing θ -norm, the doubly soft regularized regression model adjusts the sparsity of our model by choosing different θ . Compared with existing methods, ANIMC has three unique advantages: 1) it is a soft algorithm to adjust our framework in different scenarios, thereby improving its generalization ability; 2) it automatically learns a proper weight for each view, thereby reducing the influence of noises; 3) it performs doubly soft regularized regression that aligns the same instances in different views, thereby decreasing the impact of missing instances. Extensive experimental results demonstrate its superior advantages over other state-of-the-art methods.

Index Terms—Noisy and incomplete multi-view clustering, soft auto-weighted strategy, doubly soft regularized regression.

I. INTRODUCTION

REAL-WORLD image data [1], [2] are often collected from different sources or represented by different views, which are called *multi-view data*¹ [3]–[5]. For example, the collected images [6]–[8] can be represented by different visual descriptors (views) [9]–[13], like CTM [14]–[16], GIST [17]–[19], SIFT [20], etc. Integrating the information from different views can help us analyze the data in a comprehensive manner [21]–[23], which motivates the development of multi-view learning methods [24]–[27]. In the field of multi-view learning, multi-view clustering is used in more and more image

processing applications due to the ends to eliminate the high cost of time and money on labeling images. The purpose of multi-view clustering is to adaptively partition data into their respective groups by fully integrating the information from multiple views [28], rather than by simply concatenating all views into one single view for clustering. Up to present, many multi-view clustering methods have been proposed, like latent space-based methods [25], [29], graph-based methods [30]–[32], nonnegative matrix factorization (NMF) based methods [33], etc. Although most multi-view clustering methods can solve some problems in real-world applications, they still face two major problems.

One problem is the missing instances in multi-view data [34]. Most multi-view clustering methods require that each view has no missing instances. But real-world multi-view data always contain missing instances, which leads to the incomplete multi-view clustering problem. For example, in the camera network, some cameras may temporarily fail due to power outage, which will result in missing instances. As such, this incompleteness may lead to the lack of columns or rows in the view matrix, which will result in the degradation or failure of previous methods.

Another problem is the noises in multi-view data. For instance, real-world images often contain some noises [35]–[37]. For instance, many landscape images often contain fog and rain, which are common noises in image processing. If we directly process these landscape images, these noises may cause deviations in the calculation, which will damage the clustering performance.

To tackle the first problem, several incomplete multi-view clustering methods have been proposed [38]–[42]. But they ignore the influence of noises (i.e., the second problem), which are ubiquitous in the real-world image clustering tasks [43], [44]. These noises will affect the clustering calculation, which may lead to inaccurate clustering results. Specifically, these methods directly conduct the procedure by constructing a basis matrix for each view and a common latent subspace for all views that are rarely modified. But real-world datasets always contain noises that result in unreliable basis matrices and unavailable latent subspace, which impairs the clustering performance.

For the second problem, a simple solution is to assign a proper weight to each view [31]. However, in most image processing tasks, previous incomplete multi-view clustering methods [38]–[42] are difficult to weight different views due to the following challenges:

- The combined effects of noises and incompleteness make

X. Fang is with the School of Computer Science and Technology, Huazhong University of Science and Technology, Wuhan 430074, China (e-mail: xfang9508@gmail.com).

Y. Hu is with the School of Computer Science and Technology, Huazhong University of Science and Technology, Wuhan 430074, China (e-mail: yuchonghu@hust.edu.cn).

P. Zhou is with the Hubei Engineering Research Center on Big Data Security, School of Cyber Science and Engineering, Huazhong University of Science and Technology, Wuhan 430074, China (e-mail: panzhou@hust.edu.cn).

X.-Y. Liu is with the Department of Electrical Engineering, Columbia University, New York, NY 10027 USA (e-mail: xl2427@columbia.edu).

D. O. Wu is with the Department of Electrical and Computer Engineering, University of Florida, Gainesville, FL 32611 USA (e-mail: dpwu@ieee.org).

¹A brief introduction about multi-view image processing is available on Wu's homepage: http://www.wu.ece.ufl.edu/ppt/Multiview_new.pdf.

these incomplete multi-view clustering methods obtain the unsatisfactory clustering results. When we cluster these multi-view image datasets, both missing instances and noises will influence the weights of these views. The existing methods [38]–[42] are difficult to consider the effects of missing instances and noises simultaneously.

- As the missing rate increases, the availability of each view also changes. If we weight each view based on parameters, the selection of parameters for each case will have a high cost of time and it will be difficult for us to assign a proper weight to each view. To our best knowledge, it is still an open problem to select the optimal values for these parameters in different clustering tasks, which limits the application of parameter-weighted incomplete multi-view clustering methods [38]–[42].
- For different multi-view datasets, we often need to design different objective functions for clustering. Thus, a series of effective objective functions should be designed to improve the generalization ability. The generalization ability of previous methods is limited because these methods [38]–[42] are based on a single objective function.

Therefore, multi-view clustering still faces significant challenges. In this paper, we propose a novel Auto-weighted Noisy and Incomplete Multi-view Clustering (ANIMC) framework to meet these challenges. ANIMC is a joint of a *soft* auto-weighted strategy and a doubly *soft* regularized regression model². First, by designing adaptive semi-regularized nonnegative matrix factorization (adaptive semi-RNMF), we propose a soft auto-weighted strategy to assign a *proper* weight to each view. Second, by devising θ -norm, we perform doubly soft regularized regression to align the same instances in different views. The main contributions of our proposed ANIMC algorithm are summarized as follows:

- To the best of our knowledge, ANIMC is the *first* auto-weighted soft framework for noisy and incomplete multi-view clustering. The soft framework can keep high-level clustering performance on different datasets, which verifies its strong generalization ability.
- By proposing adaptive semi-RNMF, ANIMC adaptively assigns a proper weight to each view, which diminishes the effect of noises. Also, ANIMC adds a soft boundary to the soft auto-weighted strategy, which balances the influence of noises and missing instances.
- By performing a doubly soft regularized regression model based on θ -norm, ANIMC aligns the same instances in all views, which decreases the impact of missing instances. Besides, different θ can be chosen to adjust the sparsity of the model.
- Experimental results on four real-world datasets show that ANIMC outperforms state-of-the-art methods significantly. Moreover, by making the falling direction of the objective function closer to the gradient direction, ANIMC tremendously accelerates the convergence speed by a four-step alternating iteration procedure.

The rest of the paper is organized as follows. Related work is covered in Section II. The background is described

in Section III. The proposed ANIMC framework is designed in Section IV. Experiments and analysis are reported in Section V. We conclude the paper in Section VI.

II. RELATED WORK

Since the most relevant work for our research is incomplete multi-view clustering, we will review some incomplete multi-view clustering algorithms in this section. Up to now, many incomplete multi-view clustering algorithms have been proposed [38]–[42]. These algorithms can be classified into two categories: incomplete two-view clustering and incomplete multi-view clustering with more than two views.

(i) Incomplete two-view clustering aims to cluster incomplete data with two views and the related algorithms are PVC and IMG. As the first work for incomplete multi-view clustering, PVC [38] is proposed to learn the common and private latent spaces via NMF [45], [46] and L_1 -norm regularization. But PVC simply projects instances from each view into a common subspace and overlooks the global information among the two views. To improve the clustering performance, IMG [39] extends PVC and removes the nonnegative constraint to simplify optimization. But both PVC and IMG can only solve the problem of two-view incomplete multi-view clustering, which makes these two algorithms limited when solving incomplete multi-view clustering problems.

(ii) Incomplete multi-view clustering with more than two views aims to cluster incomplete data with more than two views and the related algorithms are MIC, DAIMC and UEAF. To solve the problem of incomplete clustering based on more than two views, MIC [40] first fills the missing instances in each incomplete view with average feature values, then learns a common latent subspace based on weighted NMF and $L_{2,1}$ -norm regularization. But MIC only simply fills the missing instances with average feature values and if we cluster the data with a relatively large missing rate, this simply filling may result in a serious deviation. To align the instance information, DAIMC [41] extends MIC via weighted semi-NMF [47] and $L_{2,1}$ -norm regularized regression. To obtain the robust clustering results, UEAF [42] performs the unified common embedding aligned with incomplete views inferring framework. Both DAIMC and UEAF rely too much on alignment information. When clustering the dataset without enough alignment information, DAIMC and UEAF always obtain unsatisfactory performance because the loss of alignment information will reduce the availability of their models.

Obviously, besides ignoring the influence of noises (see Section I), each of the above incomplete multi-view clustering algorithms has the above drawbacks. These drawbacks always lead to unsatisfactory clustering results, which limit the application of these algorithms in image processing.

III. BACKGROUND

We first define some notations throughout the paper. For a multi-view dataset $\{\mathbf{X}^{(v)}\}_{v=1}^m \in \mathbb{R}^{d_v \times n}$ with n instances and m views, we can cluster these instances into c clusters, where d_v is the feature dimension of the v -th view; $[n] \stackrel{\text{def}}{=} \{1, 2, \dots, n\}$; $\mathbf{U}^{(v)} \in \mathbb{R}^{d_v \times c}$ is the basis matrix of the v -th

²A soft model is a series of functions with similar structures.

view, $\mathbf{V} \in \mathbb{R}^{n \times k}$ is the common latent feature matrix of all the views; for any matrix \mathbf{B} , $\mathbf{B}_{i,j}$ is the element in its i -th row and j -th column, and $\mathbf{B}_{i,:}$ is its i -th row; \mathbf{I} denotes the identity matrix; $\mathbf{g}^{(v)} \in \mathbb{R}^{n \times 1}$ is an n -dimensional vector to indicate the incompleteness of the v -th view, and we diagonalize $\mathbf{g}^{(v)}$ to the diagonal matrix $\mathbf{T}^{(v)} \in \mathbb{R}^{n \times n}$; $\|\cdot\|_F$ is F-norm; $\|\cdot\|_{2,1}$ is $L_{2,1}$ -norm; $\|\cdot\|_\theta$ is θ -norm; for any number q , q^+ is its right limit; α and β are the nonnegative parameters.

A. Regularized Matrix Factorization

As a popular latent feature learning method for image processing, regularized matrix factorization (RMF) [48], [49] outperforms other latent feature learning methods based on KNN or co-clustering. For a data matrix $\mathbf{X} \in \mathbb{R}^{d \times n}$, RMF approximates \mathbf{X} with a matrix $\mathbf{V} \in \mathbb{R}^{n \times c}$ and a matrix $\mathbf{U} \in \mathbb{R}^{d \times c}$. Therefore, the objective function is as follows:

$$\min_{\mathbf{U}, \mathbf{V}} \|\mathbf{X} - \mathbf{UV}^T\|_F^2 + \alpha(\|\mathbf{U}\|_F^2 + \|\mathbf{V}\|_F^2), \quad (1)$$

where α is a nonnegative parameter. For ease of description, we name \mathbf{U} as *basis matrix* and \mathbf{V} as *latent feature matrix*.

Note that Eq. (1) is a biconvex problem. Therefore, it is unrealistic to expect an algorithm to find the global optimal solution. Similar to [48], [49], we can update \mathbf{U} and \mathbf{V} by

- (i) Update \mathbf{U} (while fixing \mathbf{V}) by $\mathbf{U} = \mathbf{XV}(\alpha\mathbf{I} + \mathbf{V}^T\mathbf{V})^{-1}$.
- (ii) Update \mathbf{V} (while fixing \mathbf{U}) by $\mathbf{V} = \mathbf{X}^T\mathbf{U}(\alpha\mathbf{I} + \mathbf{U}^T\mathbf{U})^{-1}$.

B. Semi-nonnegative Matrix Factorization

Since semi-nonnegative matrix factorization (semi-NMF) [47] can extract the latent feature information from the data, it has been widely used in single view clustering. For a data matrix $\mathbf{X} \in \mathbb{R}^{d \times n}$, semi-NMF approximates \mathbf{X} with a nonnegative matrix $\mathbf{V} \in \mathbb{R}^{n \times c}$ and a matrix $\mathbf{U} \in \mathbb{R}^{d \times c}$. Since \mathbf{U} can be negative, semi-NMF can handle negative input, which extends NMF. The framework of semi-NMF is

$$\begin{aligned} \min_{\mathbf{U}, \mathbf{V}} \|\mathbf{X} - \mathbf{UV}^T\|_F^2 \\ \text{s.t. } \mathbf{V}_{i,j} \geq 0, i \in [n], j \in [c]. \end{aligned} \quad (2)$$

Similar to RMF, the objective function of Eq. (2) is biconvex. [47] proposes an iterative updating algorithm to find the locally optimal solution as follows:

- (i) Update \mathbf{U} (while fixing \mathbf{V}) by $\mathbf{U} = \mathbf{XV}(\mathbf{V}^T\mathbf{V})^{-1}$.
- (ii) Update \mathbf{V} (while fixing \mathbf{U}) by

$$\mathbf{V}_{i,j} = \mathbf{V}_{i,j} \cdot \sqrt{\frac{(\mathbf{X}^T\mathbf{U})_{i,j}^+ + [\mathbf{V}(\mathbf{U}^T\mathbf{U})]_{i,j}^-}{(\mathbf{X}^T\mathbf{U})_{i,j}^- + [\mathbf{V}(\mathbf{U}^T\mathbf{U})]_{i,j}^+}}, \quad (3)$$

where $\mathbf{B}_{i,j}^+ = (|\mathbf{B}_{i,j}| + \mathbf{B}_{i,j})/2$, $\mathbf{B}_{i,j}^- = (|\mathbf{B}_{i,j}| - \mathbf{B}_{i,j})/2$, where \mathbf{B}^+ is the positive part of a matrix \mathbf{B} and \mathbf{B}^- is the negative part of a matrix \mathbf{B} . Note that for any $\mathbf{B}_{i,j}$, we have $\mathbf{B}_{i,j}^+ > 0$ and $\mathbf{B}_{i,j}^-$. Thus, the separate can ensure the square root in Eq. (3) is meaningful. In addition, $\mathbf{B}_{i,j}^+ + \mathbf{B}_{i,j}^- = |\mathbf{B}_{i,j}|$ and $\mathbf{B}_{i,j}^+ - \mathbf{B}_{i,j}^- = \mathbf{B}_{i,j}$.

C. Extending to Semi-RNMF

In real-word image processing applications, we often predict picture clusters by RMF and extract the latent feature information by semi-NMF. To improve the clustering performance, a natural idea is to combine RMF and semi-NMF, so we propose the semi-RNMF framework as follows:

$$\begin{aligned} \min_{\mathbf{U}, \mathbf{V}} \|\mathbf{X} - \mathbf{UV}^T\|_F^2 + \alpha(\|\mathbf{U}\|_F^2 + \|\mathbf{V}\|_F^2) \\ \text{s.t. } \mathbf{V}_{i,j} \geq 0, i \in [n], j \in [c]. \end{aligned} \quad (4)$$

We can update \mathbf{U} (while fixing \mathbf{V}) by $\mathbf{U} = \mathbf{XV}(\alpha\mathbf{I} + \mathbf{V}^T\mathbf{V})^{-1}$.

Based on the KKT complementary condition for the non-negativity of \mathbf{V} , we can update \mathbf{V} (while fixing \mathbf{U}) by

$$\mathbf{V}_{i,j} = \mathbf{V}_{i,j} \cdot \sqrt{\frac{(\mathbf{X}^T\mathbf{U})_{i,j}^+ + [\mathbf{V}(\alpha\mathbf{I} + \mathbf{U}^T\mathbf{U})]_{i,j}^-}{(\mathbf{X}^T\mathbf{U})_{i,j}^- + [\mathbf{V}(\alpha\mathbf{I} + \mathbf{U}^T\mathbf{U})]_{i,j}^+}}. \quad (5)$$

D. Extending to Incomplete Multi-view Clustering

To solve the incomplete multi-view clustering problem, we need to extend Eq. (4). For an incomplete multi-view dataset $\{\mathbf{X}^{(v)}\}_{v=1}^m$, we assume that different views have distinct basis matrices $\{\mathbf{U}^{(v)}\}_{v=1}^m$ and a common latent feature matrix \mathbf{V} .

First, we define an n -dimensional column vector $\mathbf{g}^{(v)}$ to indicate the incompleteness:

$$\mathbf{g}_i^{(v)} = \begin{cases} 1, & \text{if the } i\text{-th instance is in the } v\text{-th view;} \\ 0, & \text{otherwise.} \end{cases} \quad (6)$$

To facilitate matrix operations, we extend $\mathbf{g}^{(v)}$ into an incomplete indicator matrix $\mathbf{G}^{(v)} \in \mathbb{R}^{d_v \times n}$:

$$\mathbf{G}_{:,i}^{(v)} = \begin{cases} 1, & \text{if the } i\text{-th instance is in the } v\text{-th view;} \\ 0, & \text{otherwise,} \end{cases} \quad (7)$$

where $\mathbf{G}_{:,i}^{(v)} = 1$ denotes that the elements in the i -th column of matrix $\mathbf{G}^{(v)}$ are all 1. Note that when the v -th view contains all the instances, the matrix $\mathbf{G}^{(v)}$ is an all-one matrix. If the v -th view miss some instances, the view matrix $\mathbf{X}^{(v)}$ will miss the corresponding columns and the corresponding columns in $\mathbf{G}^{(v)}$ will become 0, i.e., $\sum_{i=1}^n \mathbf{G}_{t,i}^{(v)} < n$ (where $t \in [d_v]$).

Second, we extend Eq. (4) to

$$\begin{aligned} \min_{\mathbf{U}^{(v)}, \mathbf{V}} \sum_v (\|\mathbf{G}^{(v)} \odot (\mathbf{X}^{(v)} - \mathbf{U}^{(v)}\mathbf{V}^T)\|_F^2 \\ + \alpha(\|\mathbf{U}^{(v)}\|_F^2 + \|\mathbf{V}\|_F^2)) \\ \text{s.t. } \mathbf{V}_{i,j} \geq 0, i \in [n], j \in [c], \end{aligned} \quad (8)$$

where $\mathbf{U}^{(v)} \in \mathbb{R}^{d_v \times c}$, $\mathbf{V} \in \mathbb{R}^{n \times c}$, and \odot is the operation that multiplies two matrices by multiplying corresponding elements. But this extension is not satisfactory, we will propose a better method in the next section.

IV. PROPOSED ANIMC FRAMEWORK

By showing the drawback of the direct extension to incomplete multi-view clustering, we first present the motivation of our proposed Auto-weighted Noisy and Incomplete Multi-view Clustering (ANIMC) framework. Then we model ANIMC as the joint of a soft auto-weighted strategy and a doubly soft regularized regression model.

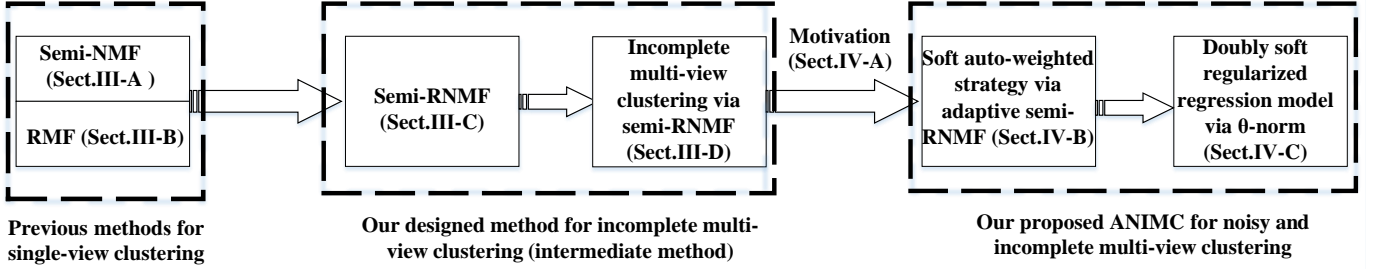


Fig. 1: The structure of the paper. “Sect.” denotes “Section”.

A. Motivation

Note that Eq. (8) is the root function to integrate different incomplete views. For different tasks, we may need different functions with stronger generalization ability than Eq. (8). A feasible idea is extending Eq. (8) to a series of exponential functions. Thus, we can rewrite Eq. (8) as

$$\begin{aligned} \min_{\mathbf{U}^{(v)}, \mathbf{V}} \sum_v (& \|\mathbf{G}^{(v)} \odot (\mathbf{X}^{(v)} - \mathbf{U}^{(v)} \mathbf{V}^T)\|_F^r \\ & + \alpha(\|\mathbf{U}^{(v)}\|_F^2 + \|\mathbf{V}\|_F^2)) \\ \text{s.t. } & \mathbf{V}_{i,j} \geq 0, i \in [n], j \in [k], \end{aligned} \quad (9)$$

where $0 < r \leq 2$. As r changes, we can obtain different exponential functions. By choosing different exponential functions, Eq. (9) can integrate all views on different tasks.

However, Eq. (9) cannot distinguish the availability of different views because Eq. (9) does not define the weight factor for each view. Intuitively, Eq. (9) only simply fills the missing instances into each view, which cannot effectively leverage the consistent information between views. If we use $\mathbf{E}^{(v)} = \mathbf{X}^{(v)} - \mathbf{U}^{(v)} \mathbf{V}^T$ to represent the noises, and $(\mathbf{G}^{(v)} \odot \mathbf{E}^{(v)})$ can represent the combination of noises and incompleteness. For a noisy and incomplete multi-view dataset, we assume that a view with more noises will have larger $\mathbf{E}^{(v)}$. Eq. (9) is difficult to deal with noises effectively because these noisy views have a greater impact on the objective function. What is worse, Eq. (9) pushes the noisy view with the lowest clustering availability hardest, which hurts the clustering performance. Therefore, we need a soft auto-weighted model to adaptively weight each view.

B. Soft Auto-weighted Strategy Via Adaptive Semi-RNMF

Different views have distinct availability, but the common latent feature matrix \mathbf{V} does not directly contain the information about the availability of each view. The information can distinguish different views and will also affect clustering results. Therefore, a clever way is to obtain the optimal \mathbf{V} and distinguish the availability of different views simultaneously through one iteration. Although Eq. (9) can integrate multiple views, it is difficult to distinguish the availability of different views after obtaining \mathbf{V} . It is because Eq. (9) does not assign weights to these views.

Therefore, we propose a novel model adaptive semi-RNMF to assign a proper weight to each view and learn optimal \mathbf{V} , simultaneously. It relies on the following two intuitive assumptions for a noisy and incomplete multi-view dataset

$\{\mathbf{X}^{(v)}\}_{v=1}^m$: (i) $\mathbf{X}^{(v)}$ is the perturbation of $\mathbf{U}^{(v)} \mathbf{V}^T$ due to noises; and (ii) incomplete views with more noises should have smaller weights. To learn optimal latent feature matrix \mathbf{V} , we can design the Lagrangian function as follows:

$$\sum_v \|\mathbf{G}^{(v)} \odot (\mathbf{X}^{(v)} - \mathbf{U}^{(v)} \mathbf{V}^T)\|_F^r + \alpha \|\mathbf{V}\|_F^2 + \zeta(\Lambda, \mathbf{V}), \quad (10)$$

where Λ is the Lagrange multiplier and $\zeta(\Lambda, \mathbf{V})$ is a proxy for the constraints. Setting the derivative of Eq. (10) w.r.t. \mathbf{V} to zero, we can obtain

$$\begin{aligned} \sum_v w_v \frac{\partial \|\mathbf{G}^{(v)} \odot (\mathbf{X}^{(v)} - \mathbf{U}^{(v)} \mathbf{V}^T)\|_F^2}{\partial \mathbf{V}} + \frac{\partial \alpha \|\mathbf{V}\|_F^2}{\partial \mathbf{V}} \\ + \frac{\partial \zeta(\Lambda, \mathbf{V})}{\partial \mathbf{V}} = \mathbf{0}, \end{aligned} \quad (11)$$

where

$$w_v = 0.5r \|\mathbf{G}^{(v)} \odot (\mathbf{X}^{(v)} - \mathbf{U}^{(v)} \mathbf{V}^T)\|_F^{0.5r-1}. \quad (12)$$

In Eq. (12), w_v depends on the target variable \mathbf{V} , so we cannot directly obtain w_v . To solve Eq. (12), we first set w_v fixed and update w_v after obtaining $\mathbf{U}^{(v)}$ and \mathbf{V} . If we fix w_v , Eq. (11) can be viewed as the solution to the following problem:

$$\begin{aligned} \min_{w_v, \mathbf{U}^{(v)}, \mathbf{V}} \sum_v (w_v \|\mathbf{G}^{(v)} \odot (\mathbf{X}^{(v)} - \mathbf{U}^{(v)} \mathbf{V}^T)\|_F^2 \\ + \alpha(\|\mathbf{U}^{(v)}\|_F^2 + \|\mathbf{V}\|_F^2)) \\ w_v = 0.5r \|\mathbf{G}^{(v)} \odot (\mathbf{X}^{(v)} - \mathbf{U}^{(v)} \mathbf{V}^T)\|_F^{0.5r-1}. \end{aligned} \quad (13)$$

But there is a case that fails Eq. (13). As the missing rate grows, the zero elements of $\mathbf{G}^{(v)}$ in Eq. (13) will also increase, and the view weight will enlarge. However, the too large weight will focus too much on the incompleteness and ignore the noises, which is difficult to reflect the impact of noises on clustering. Therefore, we need to add a soft boundary to w_v :

$$\begin{aligned} w_v = \min(0.5r \|\mathbf{G}^{(v)} \odot (\mathbf{X}^{(v)} - \mathbf{U}^{(v)} \mathbf{V}^T)\|_F^{0.5r-1}, \\ \|\mathbf{X}^{(v)} - \mathbf{U}^{(v)} \mathbf{V}^T\|_F^{-0.5}), \end{aligned} \quad (14)$$

where $0.5 \|\mathbf{X}^{(v)} - \mathbf{U}^{(v)} \mathbf{V}^T\|_F^{-0.5}$ is the boundary value of Eq. (12), which is a special case that the dataset is a complete multi-view dataset with $r = 1$. Based on function $\min(\cdot)$, $\|\mathbf{X}^{(v)} - \mathbf{U}^{(v)} \mathbf{V}^T\|_F^{-0.5}$ can reflect the effect of noises on

clustering when the missing rate is relatively large. Therefore, the final model of adaptive semi-RNMF is

$$\begin{aligned} \min_{w_v, \mathbf{U}^{(v)}, \mathbf{V}} \sum_v (w_v \|\mathbf{G}^{(v)} \odot (\mathbf{X}^{(v)} - \mathbf{U}^{(v)} \mathbf{V}^T)\|_F^2 \\ + \alpha(\|\mathbf{U}^{(v)}\|_F^2 + \|\mathbf{V}\|_F^2)) \\ w_v = \min(0.5r \|\mathbf{G}^{(v)} \odot (\mathbf{X}^{(v)} - \mathbf{U}^{(v)} \mathbf{V}^T)\|_F^{0.5r-1}, \\ \|\mathbf{X}^{(v)} - \mathbf{U}^{(v)} \mathbf{V}^T\|_F^{-0.5}) \\ \text{s.t. } \mathbf{V}_{ij} \geq 0, i \in [n], j \in [k]. \end{aligned} \quad (15)$$

Note that Eq. (15) is a soft model and we can learn different weight functions $\{w_v\}_{v=1}^m$ by changing r , which enhances its generalization ability. After fixing w_v , the Lagrangian function Eq. (10) also applies to Eq. (15). After we obtain \mathbf{V} from Eq. (15), we can update w_v , which inspires us to optimize Eq. (9) by an alternative method. After optimization, the updated \mathbf{V} is at least locally optimal. For the v -th view, $\mathbf{G}^{(v)}$ indicates the missing rate and perturbation $(\mathbf{X}^{(v)} - \mathbf{U}^{(v)} \mathbf{V}^T)$ represents noises. Through the above two aspects, w_v can effectively distinguish different views, which meets our intuitive assumptions about weight. Also, Eq. (15) updates both the optimal \mathbf{V} and w_v simultaneously. Moreover, Eq. (15) not only learns the optimal \mathbf{V} , but also distinguishes different views automatically. Besides, w_v considers the combined effects of noises and incompleteness. Therefore, we regard w_v as the weight of the v -th view.

C. Doubly Soft Regularized Regression Model Via θ -norm

Note that $\alpha(\|\mathbf{U}^{(v)}\|_F^2 + \|\mathbf{V}\|_F^2)$ (in Eq. (15)) serves as the regular term of $\mathbf{U}^{(v)}$ and \mathbf{V} . As for $w_v \|\mathbf{G}^{(v)} \odot (\mathbf{X}^{(v)} - \mathbf{U}^{(v)} \mathbf{V}^T)\|_F^2$ (in Eq. (15)), it is used to fill missing instances into the view matrix. In most cases, the filling strategy is difficult to achieve good results because it cannot effectively use the information of the presented instances to complete the view matrix. In the field of statistics, regularized regression is an efficient tool for matrix completion on real-world incomplete data. To decrease the impact of missing instances, we try to design a doubly regularized regression model to cluster noisy and incomplete multi-view data. Based on the model, we attempt to push the latent feature matrix \mathbf{V} towards the consensus feature matrix (denoted by \mathbf{V}^*) and align basis matrices $\{\mathbf{U}^{(v)}\}_{v=1}^m$ to the consensus basis matrix (denoted by \mathbf{U}^*).

First, we design the F-norm regularized regression to push \mathbf{V} closer to \mathbf{V}^* . To measure the disagreement between \mathbf{V} and \mathbf{V}^* , we leverage the F-norm, which corresponds to Euclidean distance. Thus, we have

$$\min_{\mathbf{V}} \|\mathbf{V} - \mathbf{V}^*\|_F^2 + \eta \|\mathbf{V}\|_F^2, \quad (16)$$

where η is a nonnegative parameter.

Second, to align the basis matrices $\mathbf{U}^{(v)}$ of the same instance in different views, we adopt the following regularized regression function based on the F-norm:

$$\min_{\mathbf{U}^{(v)}, \mathbf{A}^{(v)}} \sum_v (\|\mathbf{A}^{(v)T} \mathbf{U}^{(v)} - \mathbf{U}^*\|_F^2 + \beta \|\mathbf{A}^{(v)}\|_F^2), \quad (17)$$

where $\mathbf{A}^{(v)} \in \mathbb{R}^{d_v \times c}$ is the regression coefficient matrix of the v -th view and β is a nonnegative parameter.

For a particular incomplete dataset, its $\mathbf{V}^* \in \mathbb{R}^{n \times c}$ and $\mathbf{U}^* \in \mathbb{R}^{c \times c}$ are constant. In general, they are low-rank for all the views, and the cluster number c plays an important role in clustering. For most tasks, we do not have to obtain specific \mathbf{V}^* and \mathbf{U}^* , and if the correct c is learned, we will get satisfactory clustering results. Therefore, we can find simple matrices as substitutes for \mathbf{V}^* and \mathbf{U}^* to simplify Eq. (16) and Eq. (17):

(i) Substitute for \mathbf{V}^* : since all the views share the same \mathbf{V} , \mathbf{V} contains the consistent information between different views. The available the consistent information is the guarantee of satisfactory clustering results. For different clustering tasks (e.g., different datasets, different missing rates, or different noise rates), we often have different \mathbf{V}^* . For matrix \mathbf{V} , we assume that due to the influence of noises we have $0 < \mathbf{V}_{i,j}^* < \mathbf{V}_{i,j}$. To improve the generalization ability of Eq. (16) (i.e., for different \mathbf{V}^* , we can obtain satisfactory clustering results), we should simplify Eq. (16) reasonably. For any matrix \mathbf{V}^* ($0 < \mathbf{V}_{i,j}^* < \mathbf{V}_{i,j}$), since $\lim_{\mathbf{V}_{i,j}^* \rightarrow 0^+} \|\mathbf{V} - \mathbf{V}^*\|_F = \|\mathbf{V}\|_F$, the upper limit of Eq. (16) is

$$\min_{\mathbf{V}} \|\mathbf{V}\|_F^2 + \eta \|\mathbf{V}\|_F^2. \quad (18)$$

Since Eq. (18) is the upper limit of Eq. (16), we can minimize its upper limit to ensure the availability of our method in different datasets with different \mathbf{V}^* , which illustrates the generalization ability of our algorithm. Therefore, we can shrink Eq. (16) to Eq. (18) for simplicity. Since η is nonnegative, we can transform Eq. (18) into

$$\min_{\mathbf{V}} \|\mathbf{V}\|_F^2. \quad (19)$$

(ii) Substitute for \mathbf{U}^* : for most real-world applications, after pushing the latent feature matrix towards the consensus feature matrix, we have maximized the consistent information between different views. When performing the regularized regression on \mathbf{U}^* , we only need to cluster n instances into c clusters. Thus, we prefer to obtain an effective c rather than a specific \mathbf{U}^* . Since \mathbf{U}^* is a c dimensional square matrix, we can leverage a c -dimensional identity matrix \mathbf{I} as an alternative to \mathbf{U}^* ³. Therefore, we can rewrite Eq. (17) as

$$\min_{\mathbf{U}^{(v)}, \mathbf{A}^{(v)}} \sum_v (\|\mathbf{A}^{(v)T} \mathbf{U}^{(v)} - \mathbf{I}\|_F^2 + \beta \|\mathbf{A}^{(v)}\|_F^2). \quad (20)$$

However, the regularized regression based on F-norm is difficult to learn the sparse $\mathbf{U}^{(v)}$ and \mathbf{V} for clustering. Because F-norm cannot select features across all data points with joint sparsity. To obtain a more robust regularized regression model, we design a doubly soft regularized regression model based on θ -norm.

For any matrix \mathbf{B} , its F-norm is defined as

$$\|\mathbf{B}\|_F = \sqrt{\sum_i \sum_j \mathbf{B}_{i,j}^2}. \quad (21)$$

³The forms of different alternatives have little effect on the clustering performance and we choose \mathbf{I} as the alternative for simplicity.

Inspired by Eq. (21), we define the θ -norm of matrix \mathbf{B} as

$$\|\mathbf{B}\|_\theta = \sum_i \frac{(1+\theta)(\sum_j \mathbf{B}_{i,j}^2)^2}{1+\theta \sum_j \mathbf{B}_{i,j}^2}, \quad (22)$$

where we can choose proper θ according to our needs. Based on matrix \mathbf{B} , we design a diagonal matrix \mathbf{D}_B defined as

$$\mathbf{D}_{B,i,i} = \frac{2+\theta(\sum_j \mathbf{B}_{i,j}^2+2)+\theta^2 \sum_j \mathbf{B}_{i,j}^2}{\theta^2(\sum_j \mathbf{B}_{i,j}^2)^2+2\theta \sum_j \mathbf{B}_{i,j}^2+1}. \quad (23)$$

Theorem 1. For any matrix $\theta > 0$, we have

$$\frac{\partial \|\mathbf{B}\|_\theta}{\partial \mathbf{B}} = \mathbf{D}_B \mathbf{B}. \quad (24)$$

Proof.

$$\begin{aligned} \frac{\partial \|\mathbf{B}\|_\theta}{\partial \mathbf{B}_{i,:}} &= \frac{\partial((1+\theta)\|\mathbf{B}_{i,:}\|_2^2/(1+\theta\|\mathbf{B}_{i,:}\|_2))}{\partial \mathbf{B}_{i,:}} \\ &= \frac{2+\theta(\|\mathbf{B}_{i,:}\|_2+2)+\theta^2\|\mathbf{B}_{i,:}\|_2}{\theta^2\|\mathbf{B}_{i,:}\|_2^2+2\theta\|\mathbf{B}_{i,:}\|_2+1} \mathbf{B}_i = \mathbf{D}_{B,i,i} \mathbf{B}_{i,:}. \end{aligned} \quad (25)$$

□

θ -norm has the following characteristics:

- 1) θ -norm is nonnegative and global differentiable;
- 2) when $\theta \rightarrow \infty$, we have $\|\mathbf{B}\|_\theta \rightarrow \|\mathbf{B}\|_{2,1}$ and $\mathbf{D}_{B,i,i} \rightarrow 1/\|\mathbf{B}_{i,:}\|_2$;
- 3) when $\theta \rightarrow 0$, we have $\|\mathbf{B}\|_\theta \rightarrow \|\mathbf{B}\|_F^2$ and $\mathbf{D}_B \rightarrow \mathbf{I}$.

As θ increases, $\|\mathbf{B}\|_\theta$ is closer to $\|\mathbf{B}\|_{2,1}$ and \mathbf{B} becomes more sparse. Since we can choose different θ to adjust the sparsity of the matrix, θ -norm can be viewed as a soft norm with a strong generalization ability. Besides, the global differentiability of θ -norm can ensure that we can learn the correct derivative, which is significant for the following optimization (see Section IV-E). Therefore, we transform Eq. (19) into

$$\min_{\mathbf{V}} \|\mathbf{V}\|_\theta. \quad (26)$$

Similarly, we transform Eq. (20) into

$$\min_{\mathbf{U}^{(v)}, \mathbf{A}^{(v)}} \sum_v (\|\mathbf{A}^{(v)T} \mathbf{U}^{(v)} - \mathbf{I}\|_F^2 + \beta \|\mathbf{A}^{(v)}\|_\theta). \quad (27)$$

Combining Eq. (26) and Eq. (27), we can obtain the doubly soft regularized regression model as follows

$$\min_{\mathbf{U}^{(v)}, \mathbf{V}, \mathbf{A}^{(v)}} \sum_v (\|\mathbf{A}^{(v)T} \mathbf{U}^{(v)} - \mathbf{I}\|_F^2 + \beta \|\mathbf{A}^{(v)}\|_\theta) + \|\mathbf{V}\|_\theta. \quad (28)$$

For the soft model Eq. (28), we can change its sparsity by adjusting θ , which improves its generalization ability.

D. Objective Function

Considering the objective for soft auto-weighted strategy (Eq. (15)) and doubly soft regularized regression model (Eq. (28)), we minimize the following problem:

$$\begin{aligned} L &= \sum_v (w_v \|\mathbf{G}^{(v)} \odot (\mathbf{X}^{(v)} - \mathbf{U}^{(v)} \mathbf{V}^T)\|_F^2 \\ &\quad + \alpha \|\mathbf{A}^{(v)T} \mathbf{U}^{(v)} - \mathbf{I}\|_F^2 + \beta \|\mathbf{A}^{(v)}\|_\theta) + \alpha \|\mathbf{V}\|_\theta \\ w_v &= \min(0.5r \|\mathbf{G}^{(v)} \odot (\mathbf{X}^{(v)} - \mathbf{U}^{(v)} \mathbf{V}^T)\|_F^{0.5r-1}, \\ &\quad \|\mathbf{X}^{(v)} - \mathbf{U}^{(v)} \mathbf{V}^T\|_F^{0.5}) \\ \text{s.t. } &\mathbf{V}_{i,j} \geq 0, i \in [n], j \in [k], \end{aligned} \quad (29)$$

Algorithm 1 ANIMC

Input: Data matrices for noisy and incomplete views $\{\mathbf{X}^{(v)}\}_{v=1}^m \in \mathbb{R}^{d_v \times n}$, indicator matrix $\{\mathbf{G}^{(v)}\}_{v=1}^m \in \mathbb{R}^{d_v \times n}$, parameters α, β , cluster number c .

Initialize regression coefficient matrix $\mathbf{A}^{(v)}$, basis matrix $\mathbf{U}^{(v)}$, view weight $w_v = 1/m$ for each view

Initialize common latent feature matrix \mathbf{V} .

Initialize iteration time $i = 0$, maximum iteration time i_{\max} .

while Eq. (29) does not converge && $i \leq i_{\max}$ **do**

Update $\mathbf{U}^{(v)}$ by Eq. (31);

Update $\mathbf{A}^{(v)}$ by Eq. (38);

Update \mathbf{V} by Eq. (42);

Update w_v by Eq. (14);

$i = i + 1$;

end while

Output: $\{\mathbf{A}^{(v)}\}_{v=1}^m, \{\mathbf{U}^{(v)}\}_{v=1}^m, \{w_v\}_{v=1}^m, \mathbf{V}$ and clustering results.

where α and β are the nonnegative parameters. For the objective function Eq. (29), our experiments will show its effectiveness and efficiency.

E. Optimization

Since Eq. (29) is not convex for all the variables simultaneously, inspired by Augmented Lagrange Multiplier (ALM) method [50], we design a four-step alternating iteration procedure to optimize it:

Step 1. Updating $\mathbf{U}^{(v)}$. Fixing the other variables, we need to minimize the following problem:

$$\begin{aligned} L(\mathbf{U}^{(v)}) &= w_v \|\mathbf{G}^{(v)} \odot (\mathbf{X}^{(v)} - \mathbf{U}^{(v)} \mathbf{V}^T)\|_F^2 \\ &\quad + \alpha \|\mathbf{A}^{(v)T} \mathbf{U}^{(v)} - \mathbf{I}\|_F^2. \end{aligned} \quad (30)$$

We can obtain $\mathbf{U}^{(v)}$ by setting the derivative of $L(\mathbf{U}^{(v)})$ w.r.t. $\mathbf{U}^{(v)}$ to zero as follows:

$$\begin{aligned} \frac{\partial L(\mathbf{U}^{(v)})}{\partial \mathbf{U}^{(v)}} &= 2w_v \mathbf{G}^{(v)} \odot (\mathbf{X}^{(v)} - \mathbf{U}^{(v)} \mathbf{V}^T) \mathbf{V} \\ &\quad + 2\alpha \mathbf{A}^{(v)} (\mathbf{A}^{(v)T} \mathbf{U}^{(v)} - \mathbf{I}) = \mathbf{0}. \end{aligned} \quad (31)$$

The Eq. (31) is the Sylvester equation w.r.t. $\mathbf{U}^{(v)}$ [51]. Based on d_v and c , we can divide Eq. (31) into two cases to facilitate the solution

Theorem 2. For the v -th view, denote $\mathbf{E}^{(v)} = \mathbf{X}^{(v)} - \mathbf{U}^{(v)} \mathbf{V}^T$, and we have $\mathbf{G}^{(v)} \odot \mathbf{E}^{(v)} = \mathbf{E}^{(v)} \mathbf{T}^{(v)}$.

Proof. For $\mathbf{G}^{(v)} \odot \mathbf{E}^{(v)}$, we have

$$(\mathbf{G}^{(v)} \odot \mathbf{E}^{(v)})_{i,j} = \begin{cases} \mathbf{E}_{i,j}^{(v)}, & \text{if instance } j \text{ is in view } v; \\ 0, & \text{otherwise.} \end{cases} \quad (32)$$

For $\mathbf{E}^{(v)} \mathbf{T}^{(v)}$, we have

$$(\mathbf{E}^{(v)} \mathbf{T}^{(v)})_{i,j} = \begin{cases} \mathbf{E}_{i,j}^{(v)}, & \text{if instance } j \text{ is not in view } v; \\ 0, & \text{otherwise.} \end{cases} \quad (33)$$

Note that $\mathbf{G}^{(v)} \odot \mathbf{E}^{(v)}$ and $\mathbf{E}^{(v)} \mathbf{T}^{(v)}$ have the same size. Besides, $(\mathbf{G}^{(v)} \odot \mathbf{E}^{(v)})_{i,j} = (\mathbf{E}^{(v)} \mathbf{T}^{(v)})_{i,j}$ in all cases, which proves Theorem 2. \square

(i) When both d_v and c are small, based on Theorem 2, we can update $\mathbf{U}^{(v)}$ by

$$\text{vec}(\mathbf{U}^{(v)}) = [\mathbf{I} \otimes ((w_v \mathbf{V}^T \mathbf{T}^{(v)} \mathbf{V}) \otimes \mathbf{I} + \alpha \mathbf{A}^{(v)} \mathbf{A}^{(v)T})]^{-1} \text{vec}(\alpha \mathbf{A}^{(v)} + w_v \mathbf{X}^{(v)} \mathbf{T}^{(v)} \mathbf{V}), \quad (34)$$

where $\text{vec}(\cdot)$ is the vectorization operation; \otimes is the Kronecker product; $\mathbf{T}^{(v)} \in \mathbb{R}^{n \times n}$ is the corresponding diagonal matrix of vector $\mathbf{g}^{(v)}$.

(ii) When both d_v and c are large, the solution is solved by a conjugate gradient [52]. For ease of calculation, Eq. (31) can be approximated as the Lyapunov equation [53].

Step 2. Updating $\mathbf{A}^{(v)}$. Fixing the other variables, we need to minimize the following problem:

$$L(\mathbf{A}^{(v)}) = \alpha \|\mathbf{A}^{(v)T} \mathbf{U}^{(v)} - \mathbf{I}\|_F^2 + \beta \|\mathbf{A}^{(v)}\|_\theta. \quad (35)$$

We can obtain $\mathbf{A}^{(v)}$ by setting the derivative of $L(\mathbf{A}^{(v)})$ w.r.t. $\mathbf{A}^{(v)}$ to zero as follows:

$$\alpha \mathbf{U}^{(v)} \mathbf{U}^{(v)T} \mathbf{A}^{(v)} - \mathbf{U}^{(v)} + \beta \mathbf{D}_A^{(v)} \mathbf{A}^{(v)} = \mathbf{0}. \quad (36)$$

By solving Eq. (36), $\mathbf{A}^{(v)}$ can be updated by

$$\mathbf{A}^{(v)} = [\alpha \mathbf{U}^{(v)} \mathbf{U}^{(v)T} + \beta \mathbf{D}_A^{(v)}]^{-1} \mathbf{U}^{(v)}. \quad (37)$$

In most image processing applications, $\mathbf{U}^{(v)}$ has a large number of rows and a small number of columns and $(\mathbf{U}^{(v)} \mathbf{U}^{(v)T} + \beta \mathbf{D}_A^{(v)})$ is close to singular, so we can use the Woodbury matrix identity [54] to simplify the calculation. Thus, we have

$$\mathbf{A}^{(v)} = \frac{\alpha}{\beta} [\mathbf{D}_A^{(v)-1} - \mathbf{D}_A^{(v)-1} \mathbf{U}^{(v)} (\mathbf{U}^{(v)T} \mathbf{D}_A^{(v)-1} \mathbf{U}^{(v)} + \beta \mathbf{I})^{-1} \mathbf{U}^{(v)T} \mathbf{D}_A^{(v)-1}] \mathbf{U}^{(v)}. \quad (38)$$

Step 3. Updating \mathbf{V} . Fixing the other variables, we need to minimize the following problem:

$$L(\mathbf{V}) = \sum_v w_v \|\mathbf{G}^{(v)} \odot (\mathbf{X}^{(v)} - \mathbf{U}^{(v)} \mathbf{V}^T)\|_F^2 + \alpha \|\mathbf{V}\|_\theta. \quad (39)$$

We can obtain \mathbf{V} by setting the derivative of $L(\mathbf{V})$ w.r.t. \mathbf{V} to zero as follows:

$$\sum_v w_v ((\mathbf{G}^{(v)} \odot \mathbf{U}^{(v)} \mathbf{V}^T)^T - (\mathbf{G}^{(v)} \odot \mathbf{X}^{(v)})^T) \mathbf{U}^{(v)} + \beta \mathbf{D}_V \mathbf{V} = \mathbf{0}. \quad (40)$$

Similar to [47], based on KKT complementary condition for the nonnegativity of \mathbf{V} , we have

$$\left(\sum_v w_v ((\mathbf{G}^{(v)} \odot \mathbf{U}^{(v)} \mathbf{V}^T)^T - (\mathbf{G}^{(v)} \odot \mathbf{X}^{(v)})^T) \mathbf{U}^{(v)} + \beta \mathbf{D}_V \mathbf{V} \right)_{i,j} \mathbf{V}_{i,j} = 0. \quad (41)$$

Therefore, \mathbf{V} can be updated by

$$\mathbf{V}_{i,j} \leftarrow \mathbf{V}_{i,j} \cdot \sqrt{\frac{[\mathbf{Z}_1]_{i,j}^+ + [\mathbf{Z}_2]_{i,j}^-}{[\mathbf{Z}_1]_{i,j}^- + [\mathbf{Z}_2]_{i,j}^+}}, \quad (42)$$

TABLE I: Statistics of the datasets

Dataset	# of instances	# of views	# of clusters
BBCSport	544	2	5
BUAA	180	2	20
Digit	2000	5	10
Scene	2688	4	8

where $\mathbf{Z}_1 = \sum_v w_v (\mathbf{G}^{(v)} \odot \mathbf{X}^{(v)})^T \mathbf{U}^{(v)}$ and $\mathbf{Z}_2 = \sum_v w_v (\mathbf{G}^{(v)} \odot \mathbf{U}^{(v)} \mathbf{V}^T)^T \mathbf{U}^{(v)} + \alpha \mathbf{D}_V \mathbf{V}$.

In Step 1 and Step 3, we often need to normalize $\mathbf{U}^{(v)}$ and \mathbf{V} to ensure the accuracy of the updating rules [40], so $\mathbf{U}^{(v)}$ and \mathbf{V} can be normalized by $\mathbf{U}^{(v)} \leftarrow \mathbf{U}^{(v)} \mathbf{Q}$, $\mathbf{V} \leftarrow \mathbf{V} \mathbf{Q}^{-1}$, where \mathbf{Q} is the diagonal matrix $\mathbf{Q}_{k,k}^{(v)} = \sum_t \mathbf{V}_{t,k}$.

Step 4. Updating w_v . Fixing the other variables, we can update the variable w_v by Eq. (14).

Our proposed ANIMC algorithm is shown in Algorithm 1.

F. Convergence and Complexity

1) *Convergence Analysis:* To optimize our proposed ANIMC, we need to solve four subproblems in Algorithm 1. Each subproblem is convex and has the closed solution w.r.t corresponding variable. Thus, the objective function Eq. (29) will reduce monotonically to a stationary point, which ensures that ANIMC can at least find a locally optimal solution.

2) *Complexity Analysis:* As shown in Algorithm 1, the operations of updating four parameters ($\mathbf{U}^{(v)}$, $\mathbf{A}^{(v)}$, \mathbf{V} , and w_v) determine the computational complexity of the algorithm. Assume i is the number of iterations, the time complexities of updating $\mathbf{U}^{(v)}$, $\mathbf{A}^{(v)}$, \mathbf{V} and w_v are respectively $O(d_v^2 c + n(d_v + c))$, $O(c(d_v^2 + c^2))$, $O(ic(nd_v + cd_v + nc))$ and $O(nc^2)$. Since $c \ll \min(d_v, n)$ in most image processing applications, the total complexity is $O(\max(d_v in(ci + d_v^2)))$.

V. EXPERIMENTS AND ANALYSIS

A. Datasets

To evaluate the effectiveness of our proposed ANIMC algorithm in real-world clustering tasks, we conduct experiments on four real-world multi-view datasets as follows: BBCSport⁴, BUAA [55], Digit⁵ and Scene [56], whose statistics are summarized in Table I. Note that BUAA, Digit and Scene are multi-view image datasets, so we perform clustering on these image datasets to analyze the capabilities of ANIMC in image clustering. BBCSport is a text dataset and we cluster it to analyze the generalization ability of ANIMC. The detailed information of these datasets is as follows:

BBCSport: The original BBCSport dataset contains 737 documents (instances) about the sport news articles collected from the BBC Sport website. These documents are described by 2-4 views and categorized into 5 clusters. In our experiments, we choose a subset with 544 instances and two views.

BUAA (BUAA-visnir face dataset): For the dataset, two types (views) of images, i.e., visual images (VIS) and near-infrared images (NIR) are regarded as the two views of persons. Following the experimental settings in [42], we

⁴<http://mlg.ucd.ie/datasets/segment.html>.

⁵<http://archive.ics.uci.edu/ml/datasets.html>.

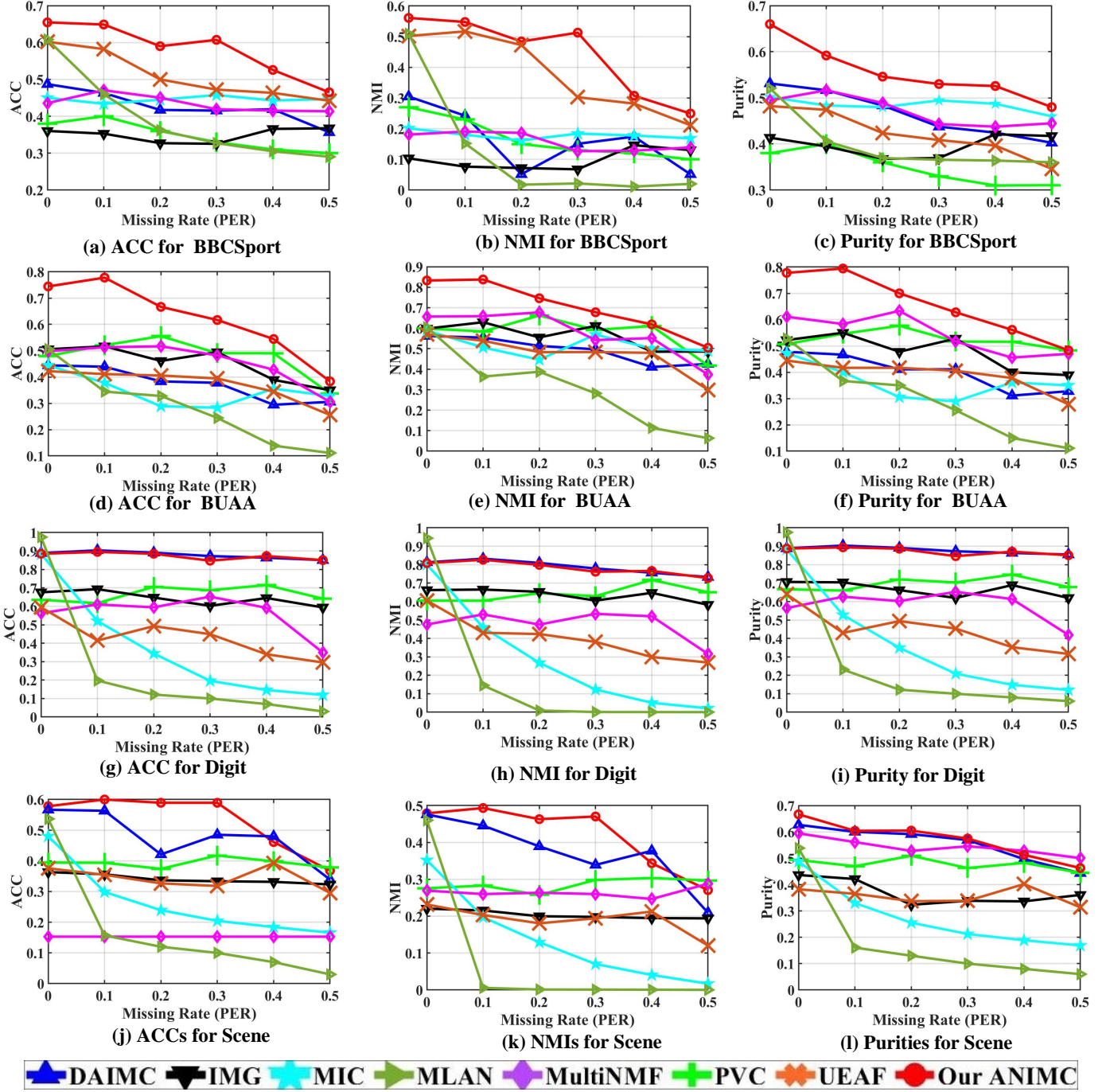


Fig. 2: Incomplete multi-view clustering results on various four datasets.

implement experiments on its subset with 180 instances and 10 clusters.

Digit (Handwritten digit dataset): Following the experimental settings in [40], we conduct the experiments on the multi-view handwritten dataset with 2000 instances and 10 digits (corresponding to 10 clusters), i.e., 0-9. In our experiments, we choose five views, i.e., 240-dimension pixel average feature in 2×3 windows (PIX), 76-dimension Fourier coefficients feature (FOU), 216-dimension profile correlations feature (FAC), 64-dimension Karhunen-Loeve coefficients feature (KAR) and 47-dimension Zernike moments feature (ZER).

Scene (Outdoor Scene dataset): Following the settings in [57], the dataset has 2688 images (instances) consisting of 8 clusters. For each image, we extract four feature vectors (views) including 512-dimension GIST, 432-dimension color moment (COL), 256-dimension HOG and 48-dimension LBP.

B. Compared Methods

We compare our proposed ANIMC framework with seven state-of-the-art methods: 1) **DAIMC** [41] extends MIC via weighted semi-NMF and $L_{2,1}$ -norm regularized regression. 2) **IMG** [39] extends PVC via a graph Laplacian term. 3)

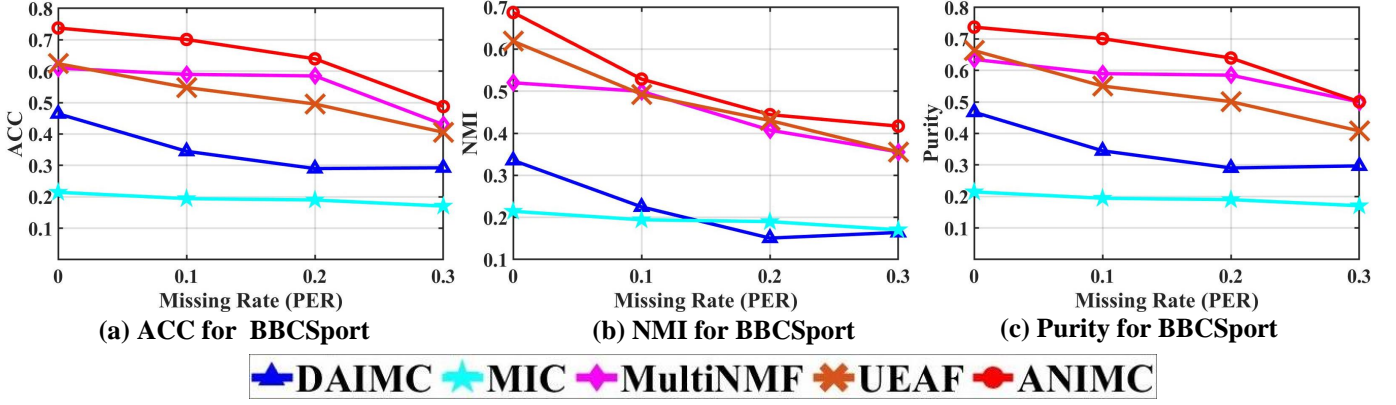


Fig. 3: Noisy and incomplete multi-view clustering on Digit.

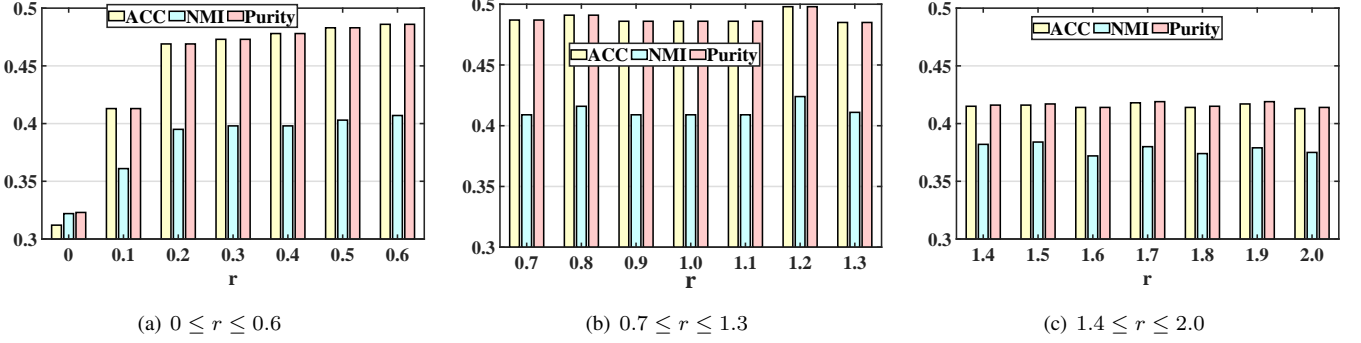


Fig. 4: Noisy and incomplete multi-view clustering with different r on Digit.

MIC [40] extends PVC via weighted NMF and $L_{2,1}$ -norm regularization. 4) **MLAN** [43] is a self-weighted framework for complete multi-view clustering. By learning the optimal graph, it performs clustering and local structure learning simultaneously. 5) **MultiNMF** [33] is a complete multi-view clustering method, it extends NMF via learning a common latent subspace. 6) **PVC** [38] learns a common latent subspace and a private latent subspace for the aligned instances and the unaligned instances, respectively. 7) **UEAF** [42] learns a consensus representation for all views by extending MIC.

For MultiNMF and MLAN, they cannot directly handle incomplete multi-view data and we fill the missing instances with average feature values, following [41]. Since IMG and PVC cannot cluster the dataset with more than two incomplete views, we use these methods on all the two-views combinations and report average results for fairness. Since our proposed ANIMC has two parameters (α and β), we adjust them to get the best performance.

Following [38] and [39], we repeat each incomplete multi-view clustering experiment 10 times to obtain the average performance. Following [40] and [41], we randomly delete some instances from each view to make these views incomplete and set the missing rate (PER) from 0 (each view is complete) to 0.5 (each view has 50% instances missing) with 0.1 as an interval. Following [42], we evaluate the experimental results by three popular metrics: Accuracy (ACC), Normalized Mutual Information (NMI), and Purity. For these metrics, the larger value represents better clustering performance. All

results of compared methods are produced by released codes, some of which may be inconsistent with published information due to different pretreatment processes. All the codes in the experiments are implemented in MATLAB R2019b and run on a Windows 10 machine with 3.30 GHz E3-1225 CPU, 64 GB main memory.

C. Results on Incomplete Multi-view Clustering

Fig. 2 shows the ACC, NMI and Purity values on four real-world datasets with various PERs. As PER increases, the performance of each method often decreases. Obviously, our proposed ANIMC significantly performs better than other state-of-the-art methods in most cases, which verifies the effectiveness and strong generalization ability of our soft framework. Especially when we cluster the BUAA dataset with PER=0.1 (Fig. 2(d), 2(e) and 2(f)), ANIMC gains large improvements around 29.31%, 18.63%, and 21.67% over the second-best algorithm in terms of ACC, NMI and Purity, respectively. Moreover, other state-of-the-art methods are difficult to maintain satisfactory clustering performance in all cases due to weak generalization ability. For example, although DAIMC can obtain a pretty clustering on Digit dataset (Fig. 2(g), 2(h) and 2(i)), it performs poorly on the BUAA dataset (Fig. 2(d), 2(e) and 2(f)).

BBCSport: Fig. 2(a), 2(b) and 2(c) show the results on the BBCSport dataset. Compared with the other methods, PVC often becomes the first worst or the second worst in most

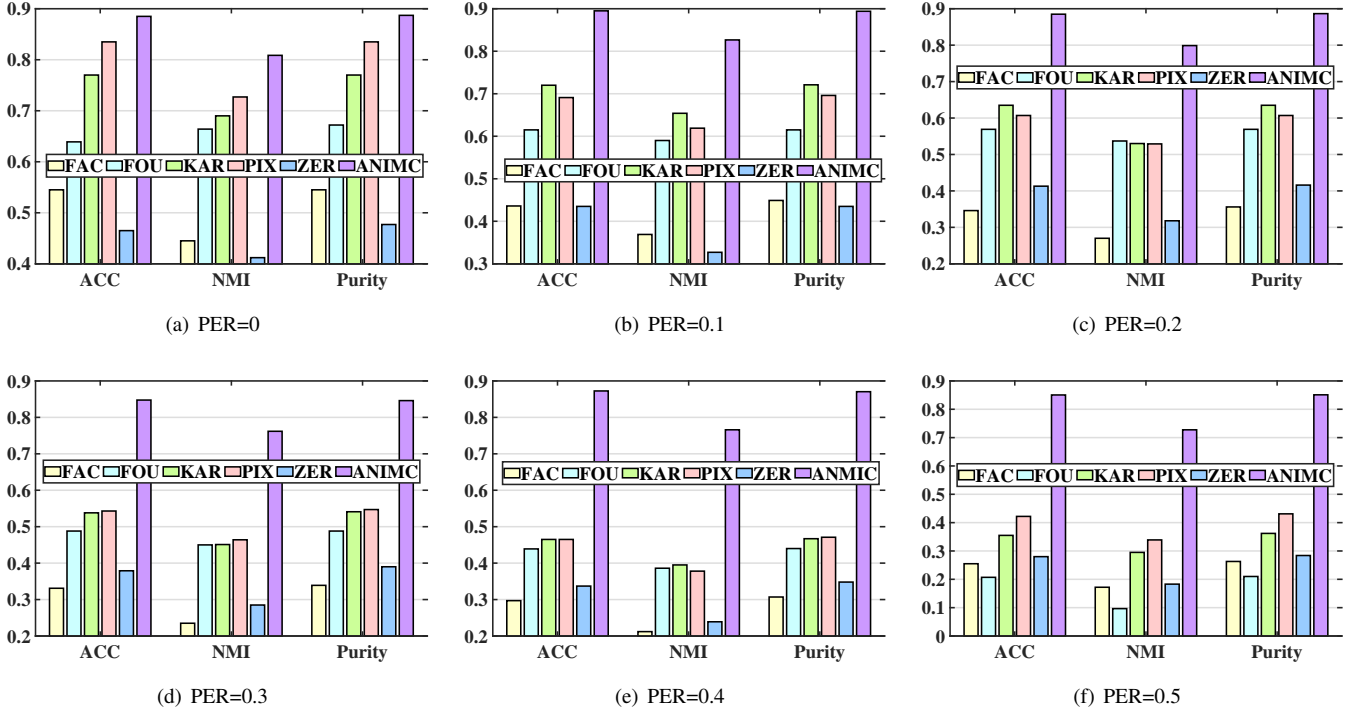


Fig. 5: Availability comparison of different views on Digit.

cases. For example, when $PER=0.1$, compared with the other methods, PVC reduces the performance at least about 4.71% in ACC, 7.58% in NMI and 0.54% in Purity, respectively. It is because PVC simply projects instances from each view into a common subspace, which overlooks the global information among the two views. Since each view of the BBCSport dataset has a large number of features, if the global information is not used effectively, it is difficult to obtain satisfactory clustering results. Thus, when the missing rate is small, the clustering results of PVC are still poor. Obviously, our proposed ANIMC outperforms all the other methods significantly for all various missing rates. Specifically, relative to MIC and DAIMC, when the missing rates are relatively small (0 to 0.3), ANIMC improves ACC by at least 21.51%, NMI by at least 20.57% and Purity by at least 3.55%; when the missing rates become larger (0.4 and 0.5), ANIMC still improves ACC by at least 1.62%, NMI by at least 7.41% and Purity by at least 1.46%. One reason for ANIMC's outstanding performance is that each view of the BBCSport dataset has a large number of features, and ANIMC can effectively integrate these features by minimizing the disagreement between the common latent feature matrix and the common consensus.

BUAA: Fig. 2(d), 2(e) and 2(f) show the results on the BUAA dataset. DAIMC and UEAF may obtain worse clustering results than PVC and IMG. For instance, when we cluster the BUAA dataset with $PER=0.3$, compared with DAIMC and UEAF, IMG raises the performance at least about 8.08% in ACC, 10.32% in NMI and 10.01% in Purity, respectively. This is mainly because the BUAA dataset contains a large number of noises that cause the learned basis matrix $U^{(v)}$ to deviate from the true value, thereby hurting the clustering

performance. ANIMC performs much better than the other methods for all various missing rates. When the missing rate is small (0 to 0.3), ANIMC raises ACC by at least 11.62%, NMI by at least 9.93% and Purity by at least 6.67%, relative to the compared methods. The reason is that our proposed adaptive semi-RNMF model can assign a smaller weight to the view with more noises (corresponding to $U^{(v)}$ with larger deviate). Thus, ANIMC can efficiently reduce the impact of noises.

Digit: Fig. 2(g), 2(h) and 2(i) show the results on the Digit dataset. Obviously, when clustering incomplete multi-view dataset (i.e., $PER > 0$), the performance of MLAN is the worst. The reason is that the missing samples will cause the nodes in the graph to fail, which makes it difficult for us to learn the optimal graph. It illustrates that these incomplete views will limit the real-world application of MLAN. Also, as PER increases, the clustering results of both MultiNMF and MIC drop significantly. Because MultiNMF and MIC only simply fill the missing samples with average feature values. This simply filling may result in a serious deviation when we cluster the data with a relatively large missing rate. Thus, this simply filling cannot effectively solve the incomplete multi-view clustering problem. Firstly, our proposed ANIMC achieves much better experimental results than UEAF, MIC, IMG, PVC and MultiNMF for all various missing rates. Especially, when the missing rates are 0.4 and 0.5, ANIMC improves ACC by at least 17.68%, NMI by at least 8.47% and Purity by at least 12.46%. Secondly, ANIMC and DAIMC have close performance, and the difference between them is less than 1%. The reason is that Digit dataset is sparse and the sparse models ($L_{2,1}$ -norm regularized regression in DAIMC

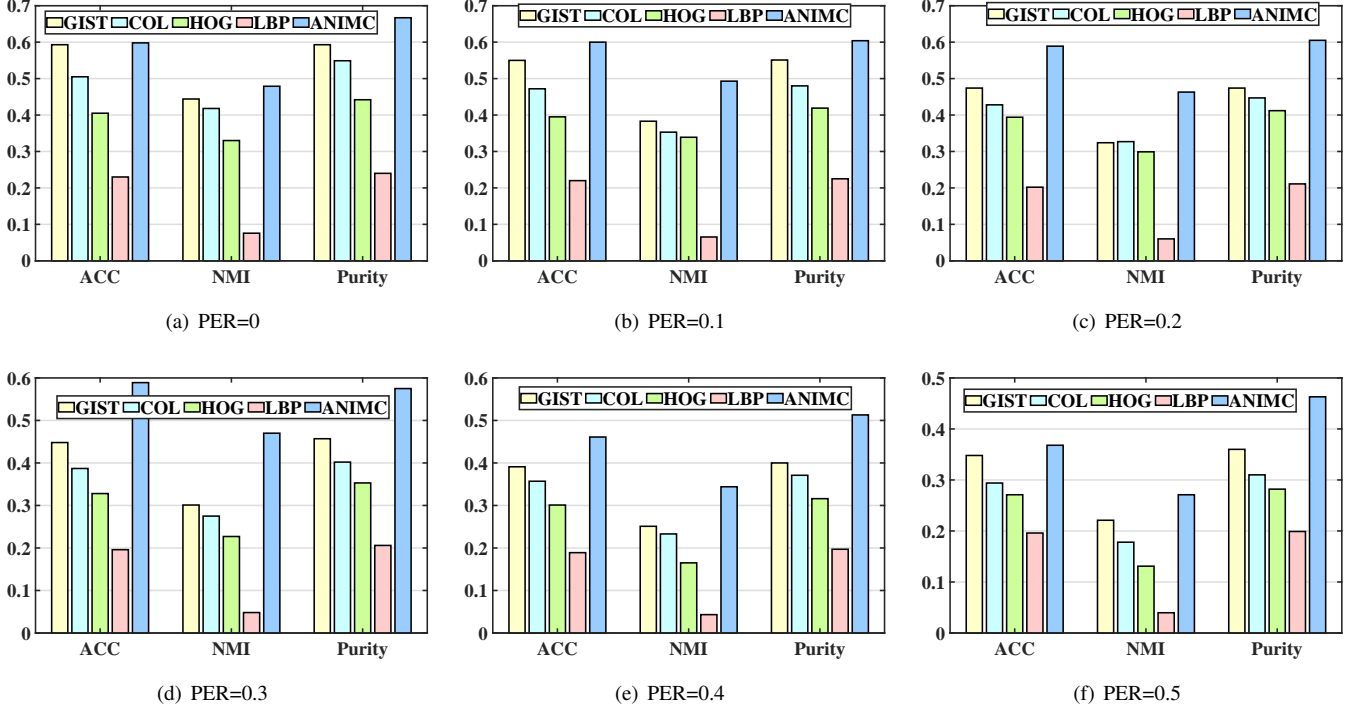


Fig. 6: Availability comparison of different views on Scene.

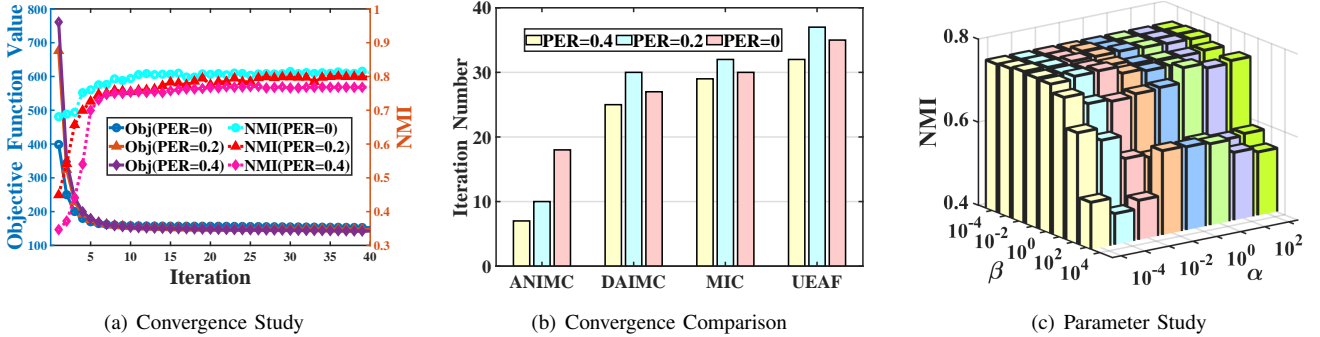


Fig. 7: Convergence and parameter study on Digit.

and doubly soft regularized regression in ANIMC) can learn the effective information of the dataset for clustering. This close performance also shows that doubly soft regularized regression is not inferior to $L_{2,1}$ -norm regularized regression.

Scene: Fig. 2(j), 2(k) and 2(l) show the results on the Scene dataset. Obviously, our proposed ANIMC outperforms the other methods in most cases. When the missing rates are 0.2 and 0.3, ANIMC raises ACC by at least 10.04%, NMI by at least 9.73% and Purity by at least 3.04%, relative to the compared methods. Note that when the missing rate is relatively small (0 to 0.3), ANIMC significantly outperforms DAIMC and UEAF because ANIMC assigns a proper weight to each view thereby decreasing the influence of noises. In addition, MultiNMF always obtains better clustering performance than PVC. The main reason is that although PVC extends MultiNMF, PVC is difficult to integrate all the views, which verifies the significance of integrating all the views.

Besides, we seek the influence of exponential function with different r , shown in Fig. 4. When we scan it in the whole range (from 0 to 2), the clustering performance keeps high-level value. Thus, r is robust to the missing rate (PER). Note that when $r = 0$ (i.e., our adaptive semi-RNMF model is removed $w_v \|G^{(v)} \odot (X^{(v)} - U^{(v)} V^T)\|_F^2 = 0$), the clustering performance is the worst, which validates the importance of the adaptive semi-RNMF model. When $0.2 \leq r \leq 1.3$, ANIMC can obtain relatively good performance. In our experiments, we choose $r = 1.2$; for θ , we set $\theta = 0.01$ for $\|V\|_\theta$ and $\theta = 100$ for $\|A^{(v)}\|_\theta$.

In summary, the performance of all the methods is analyzed as follows. Based on the auto-weighted strategy, MLAN can perform well in complete multi-view clustering tasks. But MLAN is difficult to be directly extended to incomplete multi-view clustering because missing instances will cause the graphs learned by MLAN to be unavailable. When clustering

the dataset with more than two incomplete views, PVC and IMG often achieve poor clustering results because they cannot obtain the global structure of the data. Also, real-world image processing applications often have more than three views, which limits the application of PVC and IMG. As the missing rate increases, the clustering results of both MIC and MultiNMF drop significantly because MIC and MultiNMF neglect the hidden information of the missing instances. Both DAIMC and UEAF rely too much on alignment information. When clustering the dataset without enough alignment information, they always obtain unsatisfactory clustering results because the loss of alignment information will reduce their availability. These drawbacks make these methods difficult to be widely used in real-world applications. By assigning a proper weight to each view via soft auto-weighted strategy and learning the global structure via doubly soft regularized regression model, our proposed ANIMC can obtain satisfactory performance in most cases, which shows that its potential to cluster different real-world image datasets well.

D. Noisy and Incomplete Multi-view Clustering

Gaussian noise is one of the most common noises in real-world applications, and many algorithms often use this noise to analyze their de-noising capabilities [58], [59]. Similarly, we add Gaussian noise (noisy rate=0.2, noisy variance=0.1) to the Digit dataset. Before adding noises, we normalize each view matrix of the dataset. In this section, we compare our proposed ANIMC with MultiNMF, MIC, DAIMC and UEAF.

Fig. 3 shows the noisy and incomplete multi-view clustering results on the Digit dataset. Note that both ANIMC and MultiNMF often obtain better clustering results than MIC, DAIMC and UEAF in most cases. It is because both ANIMC and MultiNMF try to align the latent feature matrix towards the consensus, which verifies the effectiveness and necessity of the doubly soft regularized regression model (in Section IV-C). Obviously, ANIMC significantly outperforms all the other methods. When $PER=0$ and $PER=0.3$, compared with these methods, ANIMC improves ACC by at least 8.46%, NMI by at least 4.32% and Purity by at least 4.00%. The main reason is that ANIMC can learn latent feature information of different views by learning optimal latent feature matrix, which decreases the influence of noises and missing instances. In particular, when $PER=0$ (i.e., the multi-view dataset is noisy and complete), ANIMC raises the clustering performance around 13.52% in ACC and 10.63% in NMI. The outstanding performance of ANIMC verifies its ability to deal with both noises and incompleteness because our adaptive semi-RNMF model can balance the impact of noises and incompleteness based on soft auto-weighted strategy (in Section IV-B). By adaptively assigning a proper weight to each noisy and incomplete view, ANIMC can distinguish the availability of different views. By assigning larger weight to the view with higher availability, we can obtain better clustering performance.

E. View Availability Study

To comprehensively analyze the availability of different views, we compare the incomplete multi-view clustering performance of each view on two datasets (Digit and Scene) with

different PERs. We compare our proposed ANIMC (multi-view clustering based on ANIMC) with single-view clustering based on ANIMC (e.g., “FAC” in Fig. 5 denotes the clustering performance using ANIMC on view FAC.). The results of the comparison are shown in Fig. 5 and Fig. 6.

Obviously, ANIMC obtains better clustering performance in all cases. For example, when $PER=0.5$, ANIMC improves ACC by at least 42.90%, NMI by at least 38.80% and Purity by at least 42.01%, which shows that ANIMC can effectively integrate different views for clustering. Moreover, different views have distinct clustering performance on single-view clustering. For instance, KAR and PIX have higher availability than FAC and ZER (see Fig. 5). Besides, as PER changes, distinct views have different relative availability. When clustering the Digit dataset, compared with FAC, FOU can obtain better performance on $PER=0$ but get worse clustering results on $PER=0.5$ (see Fig. 5). The comparison of relative availability also shows that we are difficult to choose proper parameters to weight views, which illustrates the significance of our proposed soft auto-weighted strategy (in Section IV-B).

F. Convergence Study and Parameter Sensitivity

By perform incomplete multi-view clustering on the Digit dataset, we study the convergence with different PERs, i.e., $PER=0$, $PER=0.2$ and $PER=0.4$. We set the parameters α, β as 0.1, 100, respectively. Also, we set the maximum iteration time $i_{\max} = 40$. Fig. 7(a) shows that the convergence curve and the NMI values versus the iteration number, where “Obj” denotes “objective function value”. Note that our proposed ANIMC has converged just after 20 iterations and NMI achieves the best at the convergence point for all PERs. Fig. 7(b) shows the number of iterations when ANIMC, DAIMC, MIC and UEAF converge. ANIMC converges faster than the others. The reason is that ANIMC can make the falling direction of the objective function close to the gradient direction by adaptively learning a proper weight for each view (in Eq. (15)), which shows the efficiency of our proposed soft auto-weighted strategy (in Section IV-B). Especially, when PER increases, the convergence of ANIMC is accelerated. This is because as PER increases, each incomplete view is assigned a larger weight w_v , which increases the difference of the objective function value between before and after each iteration (i.e., the declining rate of the objective function curve increases). Therefore, the objective function can converge to a stable value faster as PER increases.

For different datasets, it is difficult to adaptively select the optimal values for these parameters. Thus, we consider a simple method to obtain the optimal combination of two parameters for experiments. In terms of $\{\alpha, \beta\}$ used in our model, we conduct the parameter experiments on the Digit dataset. We set $PER=0.3$ and report the clustering performance of ANIMC versus α and β . As shown in Fig. 7(c), ANIMC not only achieves excellent clustering results but also is very robust to these parameters. Moreover, ANIMC obtains a relatively good performance when $\alpha = 0.1$ and $\beta = 100$. Therefore, we give the recommended values ($\alpha = 0.1$ and $\beta = 100$) and set the recommended values for all the datasets.

VI. CONCLUSION

In this paper, we propose a novel and soft auto-weighted framework ANIMC for noisy and incomplete multi-view clustering. ANIMC consists of a soft auto-weighted strategy and a doubly soft regularized regression model. On the one hand, the soft auto-weighted strategy is designed to automatically assign a proper weight to each view. On the other hand, the doubly soft regularized regression model is proposed to align the same instances in all views. Extensive experiments on four real-world multi-view datasets demonstrate the effectiveness of ANIMC. In the future, we will incorporate our framework with online learning algorithms for incomplete multi-view clustering on large-scale data with noises.

REFERENCES

- [1] X. Liu, J. Shi, X. Wu, and G. Zeng, "Fast first-photon ghost imaging," *Scientific reports*, pp. 1–8, 2018.
- [2] P. Yang, L. Kong, X.-Y. Liu, X. Yuan, and G. Chen, "Shearlet enhanced snapshot compressive imaging," *IEEE TIP*, 2020.
- [3] A. Blum and T. Mitchell, "Combining labeled and unlabeled data with co-training," in *COLT*. ACM, 1998, pp. 92–100.
- [4] C. Gong, D. Tao, S. J. Maybank, W. Liu, G. Kang, and J. Yang, "Multi-modal curriculum learning for semi-supervised image classification," *IEEE TIP*, 2016.
- [5] Q. Tan, G. Yu, J. Wang, C. Domeniconi, and X. Zhang, "Individuality-and commonality-based multiview multilabel learning," *IEEE Transactions on Cybernetics*, 2019.
- [6] J. Ma, X.-Y. Liu, Z. Shou, and X. Yuan, "Deep tensor admm-net for snapshot compressive imaging," in *ICCV*, 2019, pp. 10 223–10 232.
- [7] P. Zhou, C. Lu, Z. Lin, and C. Zhang, "Tensor factorization for low-rank tensor completion," *IEEE TIP*, 2017.
- [8] C. Yan, B. Gong, Y. Wei, and Y. Gao, "Deep multi-view enhancement hashing for image retrieval," *IEEE TPAMI*, 2020.
- [9] C. Wang, Z. Yan, W. Pedrycz, M. Zhou, and Z. Li, "A weighted fidelity and regularization-based method for mixed or unknown noise removal from images on graphs," *IEEE TIP*, vol. 29, pp. 5229–5243, 2020.
- [10] L. Gao, H. Yang, J. Wu, C. Zhou, W. Lu, and Y. Hu, "Recommendation with multi-source heterogeneous information," in *IJCAI*, 2018.
- [11] L. Xiao, F. Heide, W. Heidrich, B. Schölkopf, and M. Hirsch, "Discriminative transfer learning for general image restoration," *IEEE TIP*, vol. 27, no. 8, pp. 4091–4104, 2018.
- [12] R. Abdal, Y. Qin, and P. Wonka, "Image2stylegan++: How to edit the embedded images?" in *CVPR*, 2020, pp. 8296–8305.
- [13] X. Li, H. Zhang, R. Zhang, and F. Nie, "Discriminative and uncorrelated feature selection with constrained spectral analysis in unsupervised learning," *IEEE TIP*, vol. 29, pp. 2139–2149, 2020.
- [14] Z. Chen and D. Wu, "Prediction of transmission distortion for wireless video communication: Analysis," *IEEE TIP*, 2011.
- [15] D. Shao, Y. Zhao, B. Dai, and D. Lin, "Intra-and inter-action understanding via temporal action parsing," in *CVPR*, 2020, pp. 730–739.
- [16] A. Chambolle, M. J. Ehrhardt, P. Richtárik, and C.-B. Schönlieb, "Stochastic primal-dual hybrid gradient algorithm with arbitrary sampling and imaging applications," *SIAM Journal on Optimization*, 2018.
- [17] W. Min, S. Jiang, S. Wang, J. Sang, and S. Mei, "A delicious recipe analysis framework for exploring multi-modal recipes with various attributes," in *ACM MM*, 2017.
- [18] Z. Liu, S. Wang, L. Zheng, and Q. Tian, "Robust imagegraph: Rank-level feature fusion for image search," *IEEE TIP*, 2017.
- [19] Q.-Y. Jiang and W.-J. Li, "Discrete latent factor model for cross-modal hashing," *IEEE TIP*, 2019.
- [20] P. Zhou, C. Zhang, and Z. Lin, "Bilevel model-based discriminative dictionary learning for recognition," *IEEE TIP*, 2016.
- [21] C. Xu, D. Tao, and C. Xu, "A survey on multi-view learning," *arXiv preprint arXiv:1304.5634*, 2013.
- [22] S. Sun, "A survey of multi-view machine learning," *Neural Computing and Applications*, vol. 23, no. 7-8, pp. 2031–2038, 2013.
- [23] H.-C. Yang, P.-H. Chen, K.-W. Chen, C.-Y. Lee, and Y.-S. Chen, "Fade: Feature aggregation for depth estimation with multi-view stereo," *IEEE TIP*, 2020.
- [24] H. Li, J. Zhang, and C. Zong, "Implicit discourse relation recognition for english and chinese with multiview modeling and effective representation learning," *ACM TALLIP*, vol. 16, no. 3, p. 19, 2017.
- [25] C. Zhang, Q. Hu, H. Fu, P. Zhu, and X. Cao, "Latent multi-view subspace clustering," in *CVPR*, 2017, pp. 4279–4287.
- [26] X. He, Q. Liu, and Y. Yang, "Mv-gnn: Multi-view graph neural network for compression artifacts reduction," *IEEE TIP*, 2020.
- [27] X. Jia, X.-Y. Jing, X. Zhu, S. Chen, B. Du, Z. Cai, Z. He, and D. Yue, "Semi-supervised multi-view deep discriminant representation learning," *IEEE TPAMI*, 2020.
- [28] Z. Lu and Y. Peng, "Unified constraint propagation on multi-view data," in *AAAI*, 2013.
- [29] T. Zhou, C. Zhang, C. Gong, H. Bhaskar, and J. Yang, "Multiview latent space learning with feature redundancy minimization," *IEEE transactions on cybernetics*, 2018.
- [30] A. Y. Ng, M. I. Jordan, and Y. Weiss, "On spectral clustering: Analysis and an algorithm," in *NIPS*, 2002, pp. 849–856.
- [31] F. Nie, J. Li, X. Li *et al.*, "Self-weighted multiview clustering with multiple graphs," in *IJCAI*, 2017, pp. 2564–2570.
- [32] Z. Kang, X. Lu, J. Yi, and Z. Xu, "Self-weighted multiple kernel learning for graph-based clustering and semi-supervised classification," in *IJCAI*. AAAI Press, 2018, pp. 2312–2318.
- [33] J. Liu, C. Wang, J. Gao, and J. Han, "Multi-view clustering via joint nonnegative matrix factorization," in *ICDM*. SIAM, 2013.
- [34] X.-Y. Liu and X. Wang, "Ls-decomposition for robust recovery of sensory big data," *IEEE TBD*, 2018.
- [35] S. G. Chang, B. Yu, and M. Vetterli, "Wavelet thresholding for multiple noisy image copies," *IEEE TIP*, pp. 1631–1635, 2000.
- [36] H. Zhu and M. K. Ng, "Structured dictionary learning for image denoising under mixed gaussian and impulse noise," *IEEE TIP*, 2020.
- [37] M. El Helou and S. Sussstrunk, "Blind universal bayesian image denoising with gaussian noise level learning," *IEEE TIP*, 2020.
- [38] S.-Y. Li, Y. Jiang, and Z.-H. Zhou, "Partial multi-view clustering," in *AAAI*, 2014.
- [39] H. Zhao, H. Liu, and Y. Fu, "Incomplete multi-modal visual data grouping," in *IJCAI*, 2016, pp. 2392–2398.
- [40] W. Shao, L. He, and S. Y. Philip, "Multiple incomplete views clustering via weighted nonnegative matrix factorization with $l_{2,1}$ regularization," in *ECMLPKDD*. Springer, 2015, pp. 318–334.
- [41] M. Hu and S. Chen, "Doubly aligned incomplete multi-view clustering," in *IJCAI*, 2018, pp. 2262–2268.
- [42] J. Wen, Z. Zhang, Y. Xu, B. Zhang, L. Fei, and H. Liu, "Unified embedding alignment with missing views inferring for incomplete multi-view clustering," in *AAAI*, vol. 33, 2019, pp. 5393–5400.
- [43] F. Nie, G. Cai, J. Li, and X. Li, "Auto-weighted multi-view learning for image clustering and semi-supervised classification," *IEEE TIP*, 2018.
- [44] J. Gu, G. Wang, J. Cai, and T. Chen, "An empirical study of language cnn for image captioning," in *ICCV*, 2017, pp. 1222–1231.
- [45] D. D. Lee and H. S. Seung, "Learning the parts of objects by non-negative matrix factorization," *Nature*, vol. 401, no. 6755, p. 788, 1999.
- [46] D. Cai, X. He, and J. Han, "Sparse projections over graph," in *AAAI*, 2008, pp. 610–615.
- [47] C. H. Ding, T. Li, and M. I. Jordan, "Convex and semi-nonnegative matrix factorizations," *IEEE TPAMI*, vol. 32, no. 1, pp. 45–55, 2010.
- [48] W.-J. Li and D.-Y. Yeung, "Relation regularized matrix factorization," in *IJCAI*, 2009.
- [49] S. Gunasekar, B. E. Woodworth, S. Bhojanapalli, B. Neyshabur, and N. Srebro, "Implicit regularization in matrix factorization," in *NIPS*, 2017, pp. 6151–6159.
- [50] M. R. Hestenes, "Multiplier and gradient methods," *Journal of optimization theory and applications*, vol. 4, no. 5, pp. 303–320, 1969.
- [51] R. H. Bartels and G. W. Stewart, "Solution of the matrix equation $ax + xb = c$ [f4]," *Communications of the ACM*, pp. 820–826, 1972.
- [52] M. R. Hestenes, E. Stiefel *et al.*, "Methods of conjugate gradients for solving linear systems," *Journal of research of the National Bureau of Standards*, vol. 49, no. 6, pp. 409–436, 1952.
- [53] D. C. Sorensen and A. Antoulas, "The sylvester equation and approximate balanced reduction," *Linear algebra and its applications*, 2002.
- [54] N. J. Higham, *Accuracy and stability of numerical algorithms*. Siam, 2002, vol. 80.
- [55] D. Huang, J. Sun, and Y. Wang, "The buaa-visnir face database instructions," *School Comput. Sci. Eng., Beihang Univ., Beijing, China, Tech. Rep. IRIP-TR-12-FR-001*, 2012.
- [56] A. Monadjemi, B. Thomas, and M. Mirmehdi, "Experiments on high resolution images towards outdoor scene classification," tech. rep., University of Bristol, Tech. Rep., 2002.

- [57] Z. Hu, F. Nie, R. Wang, and X. Li, “Multi-view spectral clustering via integrating nonnegative embedding and spectral embedding,” *Information Fusion*, vol. 55, pp. 251–259, 2020.
- [58] G. Yuan and B. Ghanem, “ ℓ_0 tv: A sparse optimization method for impulse noise image restoration,” *IEEE TPAMI*, 2017.
- [59] M. Elhoseiny, Y. Zhu, H. Zhang, and A. Elgammal, “Link the head to the” beak”: Zero shot learning from noisy text description at part precision,” in *CVPR*. IEEE, 2017, pp. 6288–6297.